Behera, Manasa Ranjan; Murali, K.; Sundar, V.

Effect of Tidal Currents at Amphidromes on the Characteristics of N-Wave Type Tsunami

Proceedings of ninth International Conference on Hydro-Science and Engineering (ICHE 2010), IIT Madras, Chennai, India.
2 - 5 August 2010

EFFECT OF TIDAL CURRENTS AT AMPHIDROMES ON THE CHARACTERISTICS OF N-WAVE TYPE TSUNAMI

Manasa ranjan behera1[1], k. Murali[2], v. Sundar[3]

Abstract: *The disturbance due tsunami is always coupled with permanent harmonic ocean tides. The tsunami based on its time of occurrence will combine with a particular tidal phase. Thus, a coast will experience a modified water level due to a high or low tide situation. On the other hand, the tidal current at amphidromes may act as an attenuator or amplifier of the tsunami prior to its arrival at the shore. A 1D numerical study has been carried out to demonstrate the effect of amphidromic current on tsunami characteristics. A realistic N-wave profile of initial perturbation has been considered for the initiation of tsunami. This paper addresses the interaction of amphidromic current with the phase velocity of N-wave type tsunami and the subsequent run-up at the shore.*

Key words: *Tsunami, tide, N-wave, shallow water equation, amphidrome, run-up.*

1 Introduction

The tsunami generated due to submarine earthquakes, as in the case of Indian Ocean Tsunami, takes a shape of 'N' or inverse 'N', and is usually referred as N-wave (Tadepalli and Synolakis, 1994). The recent focus has been on the aspects of the modeling of tsunami in global scale to compute the run-up height and arrival time of tsunami along the coast (Behera *et al.*, 2008; Murty *et al.*, 2007). The propagation of tsunami in the ocean is a complex process as it is usually coupled with wind generated waves, internal waves, tides, etc. Among these additional environmental forces, tidal forcing is traditionally expected to play a major role in the computation of tsunami run-up height. The fairly accurate models available to compute the arrival time of tsunami are due to My Ha *et al.*, 2009; Liu *et al.*, 2009. However, accurate computation of run-up heights still remains a challenge in the present day models. Hence, the effect of co-existence of tides in general and tidal amphidromes in particular, along with the tsunami needs to be investigated for proper reproduction of the physical process. In the past, Kowalik *et al.* (2006) attempted to address the effect of tide on tsunami by investigating its interaction with tide using a 1D model, applied to the Gulf of Alaska region. It was reported that the amplification of tsunami amplitude is mainly associated with strong amplification of tsunami currents due to the nonlinear interaction of tide and tsunami. It was also mentioned that the change in the tsunami current can alter the run-up height at the shore. Hence, the run-up at the shore should be computed together for the tsunami and tide. The above aspect of the modeling is addressed in this paper. Theoretically, it is well known that the current at amphidromes is maximum and its magnitude will be higher at amphidromes in shallow waters. Thus, a critical

1 Corresponding Author, Research Fellow, email: behera_iitm@yahoo.co.in
Physical Oceanography Research Laboratory, TMSI, NUS, Singapore – 119223.
Department of Ocean Engineering, Indian Institute of Technology Madras,
Chennai, India - 600036.

investigation of the global tide-tsunami interaction in shallow waters is felt essential for a better understanding on its influence on the run-up heights. This paper aims to study the effect of tide on the propagation of N-wave type tsunami and the resulting run-up heights. The characteristics of tsunami and tide are governed by Shallow Water Equations (SWE).

2 Solution and Validation of 1D SWE model

The present investigation aims in bringing out a 1D perspective study on the tide-tsunami interaction problem to understand the complex process. For this purpose, a 1D channel has been considered. The corresponding 1D SWE in cartesian coordinates are given as

$$\frac{\partial \zeta}{\partial t}+\frac{\partial q_x}{\partial x}=0$$
$$\frac{\partial q_x}{\partial t}+\frac{\partial (u\,q_x)}{\partial x}=-\frac{H}{\rho}\frac{\partial p_a}{\partial x}-gH\frac{\partial \zeta}{\partial x}-H\frac{\partial \Omega_T}{\partial x}+\frac{\tau_{bx}}{\rho H} \quad (1)$$

where, $q_x(x,t)$ is flow discharge in X direction, that is along the length of the channel. However, $q_x = uH$, u is the average velocity in X direction. $\zeta(x,t)$ is water surface displacement from the still water level, H is the total water depth ($H = d$(still water depth) + ζ), g is the gravitational acceleration. P_a is the atmospheric pressure and Ω_T is the tide producing potential. The bottom stress (τ_b) is proportional to square of the velocity and is given by:

$$\tau_b = \rho K_b H^{-2} |q_x| q_x \quad (2)$$

The dimensionless friction coefficient K_b may be considered in the range of 1.0×10^{-3} - 3.0×10^{-3} (Dotsenko, 1998; Geist *et al.*, 2009). The linearised shallow water equations were solved by a second order accurate implicit Crank-Nicolson method on a staggered grid. The shoreline boundary of the problem domain has been imposed with a wall boundary condition. Flather condition (Carter and Merrifield, 2007) is imposed at the radiation boundary. The amplitudes and phase of the sea level and velocity at the open boundary are used as given by Kowalik *et al*. (2006). The space step and time step used for the present simulations are 1000m and 10s respectively. Simulations were carried out in line with Kowalik *et al.* (2006) for the computational domain and initial condition as shown in Fig.1 and 2.

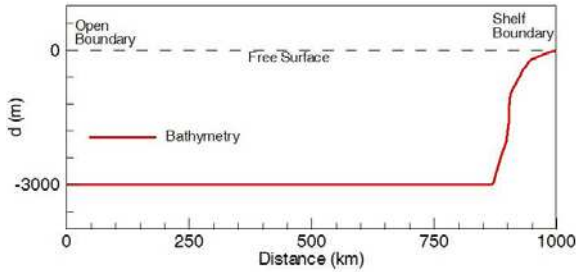

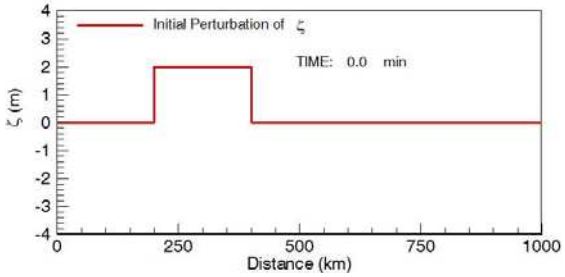

Figure 1. **Longitudinal profile of typical**

bathymetry of Gulf of Alaska. (as per

Figure 2. **Initial uniform bottom uplift**

considered for generation of tsunami.

The shelf boundary has been modelled with a wetting and drying algorithm by Kowalik *et al.* (2006). In the present study the shelf boundary is modelled as a wall boundary with a minimum water depth of 1m for computational simplicity. The computation was considered for a coupled tide and tsunami study. The tsunami was initiated into the domain with a stabilised M2 tide (after 5 tidal cycles) in such a way that it reaches the coast at the time of maximum tidal elevation. The surface elevation for coupled tsunami and tide has been recorded at the open boundary and shelf boundary. Comparison with the results of Kowalik *et al.* (2006) shown in Fig.3 proves the proper radiation of outgoing waves. The tsunami generated at the source leaves the open boundary between 62.0-63.0 hrs. After this event, only tide is observed up to about 64.3 hrs. The tsunami reflected from the shelf is observed at this time followed by the reflections originating from the shoreline boundary between 65.5 and 67.0 hrs.

It is prudent to now investigate the water surface fluctuations at the shoreline boundary. The run-up at the shoreline due to the coupled tide and tsunami from the present model compared with the results of Kowalik *et al.* (2006) is found to be reasonable as can be seen in Fig.4 except around the peak value occurring at about 63.7 hrs. This difference is produced due to the reflective boundary condition imposed at the shoreline boundary in the present model, whereas, Kowalik *et al.* (2006) have implemented a wet-dry boundary to allow the flow to flush into the dry land by reducing the instantaneous reflection of the total influx. A difference is also observed between 55 hrs and 60.5 hrs as well as between 66.5 hrs and 70 hrs. It is seen that the model of Kowalik *et al.* (2006) has not recorded any negative elevation. The wet-dry model records only positive elevation and at the dry condition it is considered as zero elevation. Thus, the results of Kowalik *et al.* (2006) does not show any negative elevation. A finite water depth has been considered at the shoreline in the present numerical model for computational ease. Thus, the negative fluctuations at the shoreline are recorded as seen in the above figure.

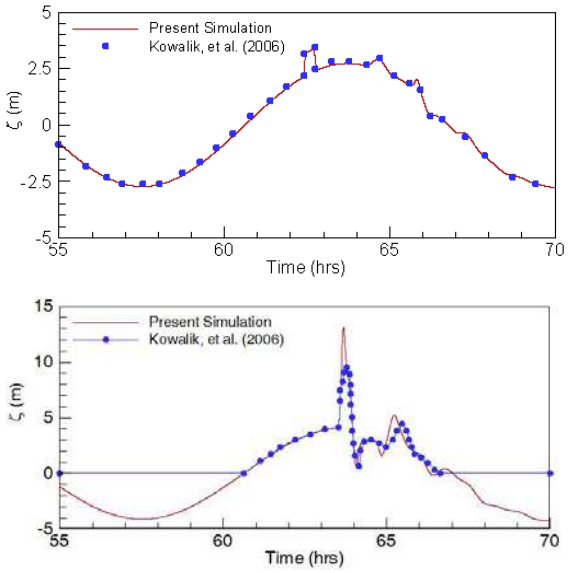

Figure 3. Comparison of elevation profiles of coupled tide and tsunami at the open boundary.

Figure 4. Comparison of elevation profiles of coupled tide and tsunami at the shelf boundary.

5 Tide-Tsunami Interaction Study

The tide in global oceans oscillates about the amphidromic points, where, the change in elevation is almost negligible at all times. By virtue of continuity of mass, the horizontal velocity due to the movement of tide is maximum at these points. When the velocity of propagating tsunami is coupled with tidal velocity at the amphidromic points, the resulting tsunami wave characteristics are expected to change. Since the tide induced velocity is at its maximum at these points, it is expected that the impact of amphidromic point will be significant. In order to understand this impact, the present 1D coupled tide-tsunami model was used.

5.1 Mechanism of wave current interaction

The interaction of tide and tsunami shall depend on the magnitude of tide induced current at the amphidromic point and the phase velocity of the tsunami. This aspect has been reasonably well understood for linear waves interacting with currents (Li and Herbich, 1984; Kaihatu, 2009). It has been long understood that the resulting doppler effect leads to a reduction in wave length and an increase in wave height for opposing currents and vice versa. Li and Herbich (1984) have quantified the magnitude of the doppler effect in terms of the non-dimensional parameter u/C and showed that the change in the wave height for u/C = ± 0.1 and 0.2 will be 15% and 30% respectively. Even though, the study carried out by Li and Herbich (1984) is for short period wind generated waves and the associated current, the concept can be extended for the present tide tsunami analysis as the physics would remain similar. In order to extend the above concept to tide-tsunami interaction, the tide considered is very long and hence the tide induced current

may be considered as u, while, the phase velocity of tsunami shall be considered as C (corresponding to the short wave). In light of the present investigations, the value of u/C for a typical amphidromic point in deep water (3000m) is of the order of 0.002. Hence, no strong coupling of tide and tsunami is expected in deep water. On the other hand, the only way the value of u/C can be altered is by moving to shallow depths, in which case, the value of u will increase significantly compared to the phase velocity of tsunami and hence will result in a higher u/C.

5.2 Amphidromes in shallow water

It is observed that the amphidromes are located at water depths as shallow as 20m as can be seen in Table1. Thus, the practical importance of amphidromes in shallow water depths is established (Bowden, 1983; Stewart, 2005) and the domain specified earlier has been considered for the tide-tsunami interaction with constant water depth of 20m. A M2 tide as specified earlier was forced at the open boundary. The typical surface elevation profiles for various phases of tide after the simulation reached a steady state in about 5 tidal cycles are shown in Fig.5. The figure also depicts the amphidromic points (or) nodes where, the elevation remains close to zero at all times. The maximum tidal velocity profiles for the different water depths (10-50m) are shown in Fig.6. It is observed that for water depths less than 20m, the harmonic profile of the velocity is not retained. In order to identify the magnitude of tide-tsunami coupling, the values of u_{max}/C for different water depths are brought out in Fig.7. It is seen that u_{max}/C is 0.14 for 20m water depth that is more than 0.1 and a strong interaction between tide and tsunami is expected as pointed out by Li and Herbich (1984).

Table 1. Amphidromic points within shelf and shoreline region.

Sl. No.	longitude (degrees)	latitude (degrees)	depth (m)
1	-88.40	60.00	175
2	-79.88	57.89	145
3	141.12	54.93	144
4	144.32	49.86	112
5	-5.80	55.28	44
6	5.52	55.33	44
7	2.70	52.40	35
8	-1.88	50.60	20

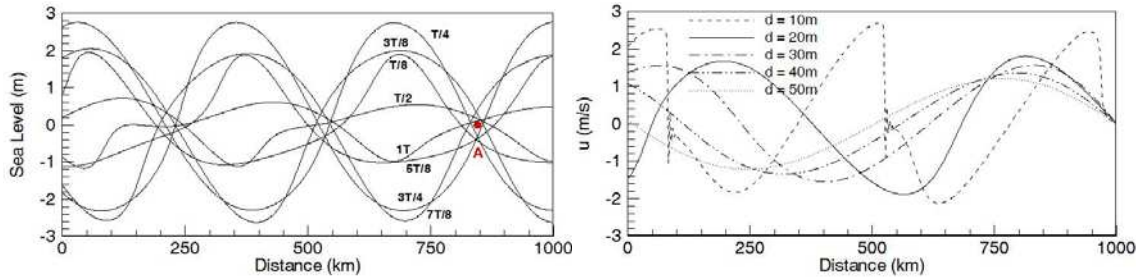

Fig 5. Surface elevation profiles depicting amphidromic points

Fig 6. Maximum tidal velocity profiles in water depths 50, 40, 30, 20 and 10m

Figure 6. Maximum tidal velocity profiles in water depths 50, 40, 30, 20 and 10m

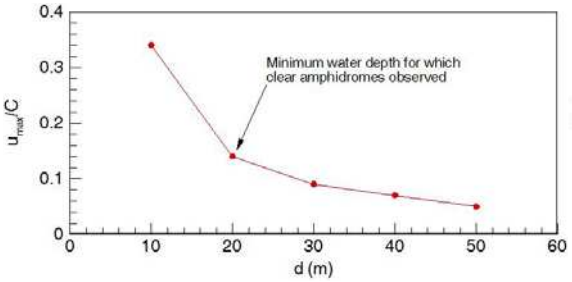

Figure 7. Variation of u_{max}/C for different water depths (ζ-tide $\approx$ 2.73m).

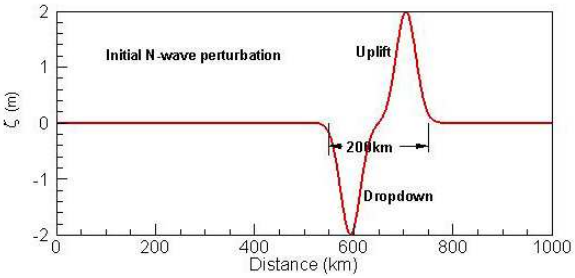

Figure 8. N-wave type perturbation considered for generation of tsunami.

5.3 N-wave tsunami profile

The tide-tsunami interaction study was carried out with a realistic initial perturbation that occurs in the ocean when a tsunami is generated due to an earthquake. The submarine earthquakes, usually generated along the fault line, distort the ocean floor by displacing the tectonic plates. The plate that moves upward generates uplift in the sea surface (positive elevation) and similarly a dropdown (negative elevation) is created by the downward moving plate. This process results in a wave profile that takes a shape of N and hence referred as N-wave (Tadepalli and Synolakis, 1994). The perturbation during the 26th December 2004 tsunami also had taken the shape of N-wave. Thus the tide tsunami interaction study was carried out with the realistic N-wave type initial perturbation of tsunami with leading crest as shown in Fig.8. The profile of N-wave was generated by using the Gaussian distribution function. Two Gaussian profiles were generated with an offset in their centers. The magnitude of one profile was reversed to generate the dropdown in the perturbation. Thus, by superposing both the profiles, the N-wave was obtained. The amplitude and base width of the perturbation can be varied by altering the variables in the Gaussian distribution function. The Gaussian distribution function can be given as;

$$f(x) = a\, e^{-\frac{(x-b)^2}{2c^2}} \tag{6}$$

where, 'a' is the crest or trough height, b is the position of the centre of the peak, and c controls the width at the base of the profile. In the present study, the N-wave is considered with crest and trough elevations of +2m and -2m respectively. The base width of N-wave was considered as 200km centered at 650km. It was positioned in such a way that the tsunami is initiated before the amphidrome A.

6 Results and discussion

The amphidrome closer to the shoreline was considered for study with tsunami being initiated before this amphidromic point. The N-wave (referred as tsunami here after) was initiated in such a way that the wave crest arrives at the amphidromic point when the tidal current is maximum following and maximum opposing at this location.

6.1 Tsunami wave profiles at amphidromic point

In order to quantify the difference between the water surface elevation due to tsunami and tide influenced tsunami (coupled tide tide-tsunami elevation – tide elevation), the respective time histories are plotted in Fig.9. The distortions in the water surface elevation is seen at the crest or trough of the tsunami for the conditions of following and opposing current when the tsunami enters the amphidromic point. In the presence of a following current, the crest elevation is found to reduce (Fig.9a), whereas, a reverse trend is observed for the tsunami propagating over an opposing current (Fig.9b). The rate of change in the tsunami elevation is found to be of the order of 15 to 20%. This effect can result in a significant change in the run-up over a beach. The early or delayed arrival of maximum elevation by 15-20min is observed in case of tsunami with leading crest for following and opposing current respectively. This difference is quite significant that needs to be considered in the design of advance warning systems or mitigation measures.

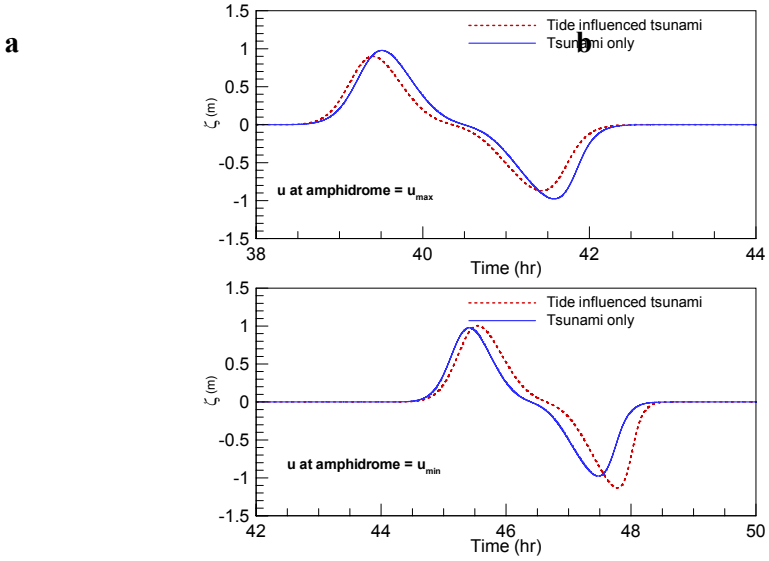

Fig 9. Time series for surface elevation of tsunami only and tide influenced tsunami with leading crest at amphidromic point. (a) u following (b) u opposing.

6.2 Tsunami run-up profiles at the shore

After having investigated the characteristics of the tsunami, while, it traverses through the amphidromic point, the effect of its deformation near the coast is investigated. In order to achieve this, the deformed tsunami was allowed to propagate and the landfall near the shore was computed. The reduced run-up heights (run-up due to coupled tide and tsunami − run-up due to only tide), for following and opposing current, are brought out in Figs.10 and 11 for tsunami with leading crest and leading trough respectively. The results show that the worst scenario will occur in the case of tsunami with leading trough interacting with opposing current and the run-up level

could be higher by about 0.4m. It is noted that the arrival time could be advanced or delayed by 25-30min depending on the following or opposing current respectively. The foregoing discussion reveals that the Doppler Effect due to the interaction of tsunami wave front with the current at amphidromic point is similar to that due to the interaction of regular wind waves with currents.

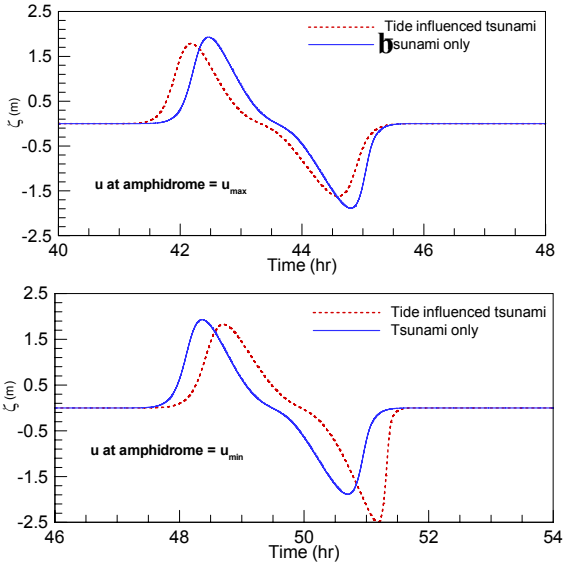

Figure 10. Time series for surface elevation of tsunami only and tide influenced tsunami with leading crest at the shore. (a) u following (b) u opposing.

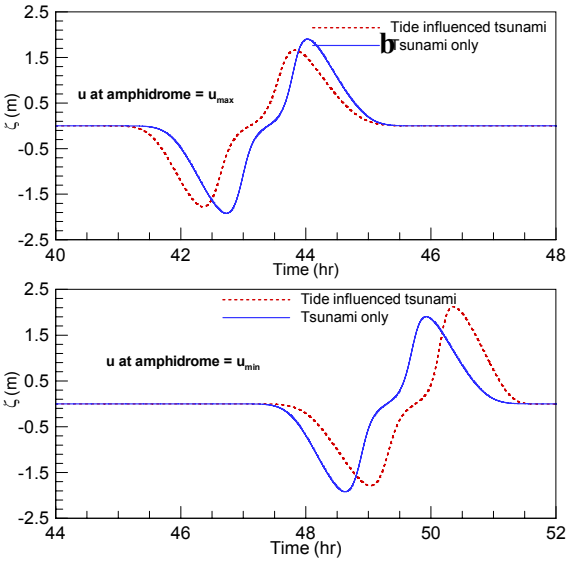

Figure 11. Time series for surface elevation of tsunami only and tide influenced tsunami with leading trough at the shore. (a) u following (b) u opposing.

6.3 Effect of amphidromic current on tsunami wave profile

The changes in the temporal characteristics of the tsunami due to the tidal velocity variation at the amphidromic point have been discussed in the previous section. However, the spatial

changes to the tsunami wave profile are not clear from the above study. Thus an attempt is made to study the changes in the wave profile at various phases of the current at amphidromic point and such changes in the tsunami profile with the crest centred at the amphidromic point are shown in Fig.12. When the tsunami arrives during the maximum velocity at amphidromic point, a forward shift is observed and consequently a reduction in the crest elevation is noticed (Fig.12a). The reduction in crest elevation is about 15-20% as depicted in the figure. The tsunami when arrives at the amphidromic point with opposing tidal velocity at that point, an increase in the wave height (by about 15-20%) and a reduction in the wave length is observed as can be seen in Fig.12b. A backward shift of the crest profile is observed with the negative velocity. Thus, the prominence of Doppler Effect in shallow water is evident.

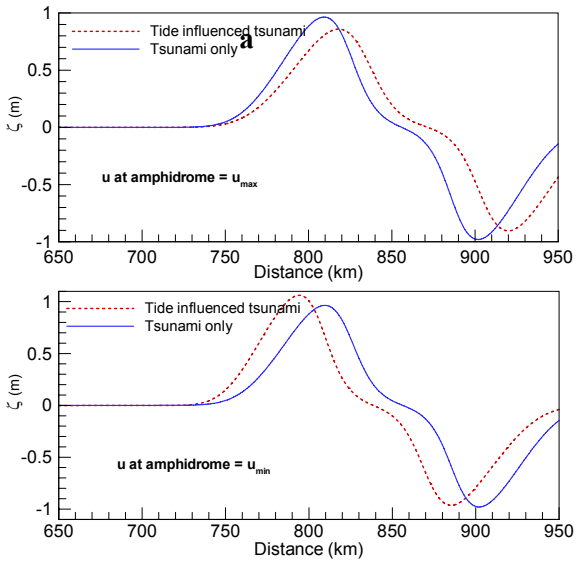

Fig 12. Profile of only tsunami and tide influenced tsunami with leading trough at amphidromic point. (a) u following (b) u opposing.

6.4 Effect of sloping shelf on run-up at the shore

The foregoing discussion brings out the effect of pure interaction of tsunami with the current at amphidromic point. However, in real scenarios the effect of shoaling due to the slope will be present. In order to bring out such realistic effect, a sloping shelf near the shore was considered as shown in Fig.13. The sloping bathymetry varies from 20m at 100km away from shore to 4m at the shore. The finite water depth of 4m was considered at the shore for computational stability. Thus, the effect of shoaling is brought into the study. The N-wave with leading trough was considered for this study, as this approximation is closer to the realistic tsunami wave. In order to achieve the effect of shoaling, the deformed tsunami at the amphidromic point was allowed to propagate over the slope and the run-up at the shore was computed. The computational set-up and details of simulation remain the same as earlier. Salient results of the study are discussed below.

The effects of wave shoaling over the sloping shelf are brought out in Fig.14. In case of following current at the amphidromic point, a reduction in the run-up and wave height of about 30% is observed for tide influenced tsunami compared to the run-up due to tsunami only

simulation (Fig.14a). This means that the superposed simulation will over predict the run-up by about 30% with respect to coupled simulation. On the other hand, an opposing current of tide at the amphidromic point, increases the run-up by about 1.3m (about 40%) for tide influenced tsunami compared to the run-up due to only tsunami simulation as can be seen in Fig.14b. Thus, the study shows that the effect of current at the amphidromic point on run-up at the shore following a sloping beach is significant and can be of the order of 30 - 40%.

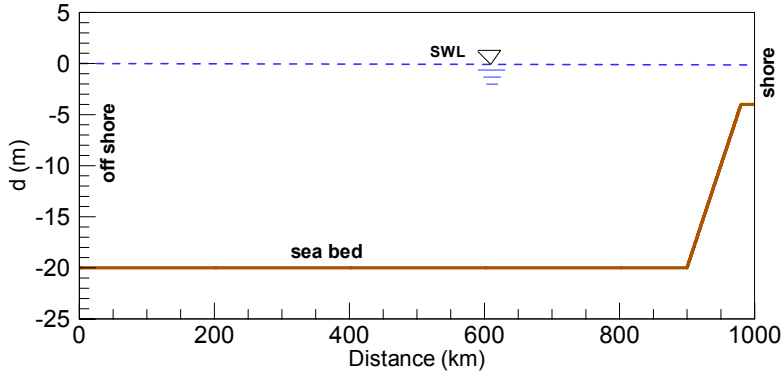

Figure 13. Longitudinal cross section of sea bed profile with a gradual slope near the shore.

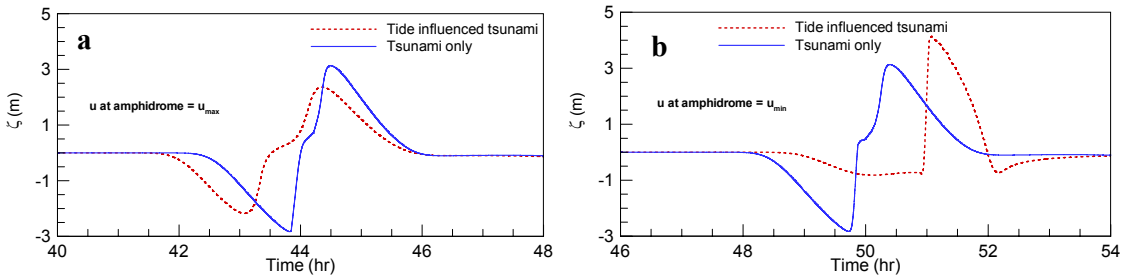

Fig 14. Maximum run-up of tide influenced tsunami and corresponding only tsunami with leading trough near the shore with a sloping beach. (a) u following (b) u opposing.

7 Conclusions

A study has been carried out to investigate the interaction of tide and N-wave type tsunami at the tidal amphidromes and the consequent run-up at the shore. A 1D linear shallow water equation model has been developed for this purpose and validated with the results of Kowalik *et al.* (2006). It was observed that the effect of amphidromes in deep water is insignificant as was also observed by Kowalik *et al.* (2006). The relative velocity parameter, u_{max}/C, which is known in the case of wave-current interaction, can be a leading parameter to suggest the level of coupling between phase velocity of tsunami and tidal current at amphidrome. For this purpose, u_{max} may be taken as the magnitude of tidal amphidromic current and C ($=\sqrt{(gh)}$) as the phase velocity of tsunami. The detailed investigations carried out at a water depth of 20m ($u_{max}/C=0.14$) reveal that the tsunami height will significantly change due to its interaction with the maximum current at the amphidromic point. The following and opposing currents results in a reduction and increase in the elevation of the wave crest respectively. The change is of an order of 15-20%. The arrival of the maximum run-up at shore depends on the phase of velocity at amphidrome at

which the tsunami arrives. The interaction with following and opposing phase leads to early or delayed arrival of maximum run-up respectively. The study suggests that the coupled tide-tsunami simulation is necessary for proper reproduction of the interaction in the shallow water and resulting run-up and arrival time of tsunami.

References

1. Behera, M.R., Murali, K., Sannasiraj, S.A. and Sundar, V. (2008), "Explicit FE modelling of Indian Ocean Tsunami using unstructured mesh", *International Journal of Ecology and Development*, Special Issue on Coastal Engineering, 10(8), 115-128.
2. Bowden, K.F. (1983), "Physical oceanography of coastal waters", *JOHN WILEY & SONS*, New York. ISBN 0-470-27505-7.
3. Carter, G.S. and Merrifield M.A. (2007), "Open boundary conditions for regional tidal simulations", *Ocean Modelling*, 18, 194-209.
4. Dotsenko, S.F (1998), "Numerical modelling of the propagation of tsunami waves in the Crimean peninsula shelf zone", *Physical Oceanography*, 9(5), 323-331.
5. Geist, E.L., Lynett, P.J. and Chaytor, J.D. (2009), "Hydrodynamic modelling of tsunami from the Currituck landslide", *Marine Geology*, 264, 41-52.
6. Kaihatu, J.M. (2009), "Application of a nonlinear frequency domain wave-current interaction model to shallow water recurrence effects in random waves", *Ocean Modelling*, 26, 190-205.
7. Kowalik, Z., Proshutinsky, T. and Proshutinsky, A. (2006), "Tide-Tsunami Interactions", *Science of Tsunami Hazards*, 24(4), 242-256.
8. Li, Y,C. and Herbich, J.B. (1984), "Wave length and celerity for interacting wave current", *Proc. 3rd Int. Offshore Mech. And Arctic Engrg.*, New Orleans, USA, 114-118.
9. Liu, P.L.F., Wang, X. and Salisbury, A.J. (2009), "Tsunami hazard and early warning system in South China Sea", *Journal of Asian Earth Sciences*, 36, 2-12.
10. Murty, T.S., Aswathanarayana, U. and Nirupama, N. (2007), "The Indian Ocean Tsunami", *Taylor & Francis Group*, London, UK.
11. My Ha, D., Tkalich, P., Soon, C.E. and Megawati, K. (2009), "Tsunami propagation scenarios in the South China Sea", *Journal of Asian Earth Sciences*, 36, 67-73.
12. Stewart, R.H. (2005), "Physical Oceanography", *Texas A & M University*.
13. Tadepalli, S. and Synolakis, C.E. (1994), "The run-up of N-waves", *Proc. Roy. Soc. London,* A445, 99-112.